PROCEEDINGS OF THE 11th INTERNATIONAL MINERAL PROCESSING SYMPOSIUM
21-23 October 2008, Belek-Antalya, Turkey

Adsorption Mechanism of Mixed Long-chain Amines and Alcohols on Silicate Minerals

A. Vidyadhar, A. Das, K. K. Bhattacharyya, Rao K. Hanumantha
Mineral Processing Division, National Metallurgical Laboratory, Jamshedpur
Lulea University of Technology, Division of Mineral Processing, Lulea, Sweden

ABSTRACT:
The mechanism of adsorption of long chain alkyl primary amines and co-adsorption of amines and alcohols on silicate minerals (quartz and feldspar) were studied using FTIR (DRIFT and IRRAS) and XPS spectroscopy methods at neutral pH 6-7. The spectroscopic data were correlated with zeta-potential and Hallimond flotation results. The influence of long chain alcohols on the adsorption of amines in mixed amine-alcohol is also examined.

The infrared studies revealed that the amine cation form strong hydrogen bonds with the surface silanol groups. The XPS spectra revealed the presence of molecular amine together with the protonated amine on silicate surface. Based on these observations, a model of successive two-dimensional and three-dimensional precipitation was suggested to explain amine adsorption on a silicate surface. The co-adsorption of long chain alcohols with amine cations leads to formation of a closer packed surface layer with synergistic enhancement of amine adsorption. The enhanced adsorption and hence higher flotation recoveries is discussed in the light of our experimental results.

Keywords: Quartz, feldspar, adsorption, flotation, zeta-potential, FTIR, XPS

1. INTRODUCTION:

The understanding of the mechanism of adsorption of long-chain alkyl amines and elucidation of the properties of the adsorbed layers is important for a variety of industrial applications. In particular, primary long-chain alkylammonium salts are most commonly used flotation collectors for beneficiation of silicates (Leja, 1982), principally because of their relatively high solubility. This problem was studied extensively by indirect methods of the measurement of contact angle, zeta-potential, surface forces and flotation recovery response during the last 60 years (Fuerstenau and Raghavan, 1980; Smith and Scott, 1990; Laskowski, 1999). Untill recently, the adsorption of amines on silicates at neutral pH has been explained mainly by the Gaudin-Fuerstenau-Somasundaran model (Gaudin and Fuerstenau, 1955; Somasundaran and Fuerstenau, 1966; Fuerstenau and Jang, 1991). Although the general mechanism of the coadsorption of long chain amines and alcohols on silicates was studied, there was no direct spectroscopic observation of coadsorption of amines and alcohols on silicates and dependence of the adsorbed layer structure

on the relationship between chain lengths of both components. However, the individual adsorption of primary amines and alcohols on quartz and albite have been studied by direct spectroscopic measurement very recently (Vidyadhar and Rao, 2007; Vidyadhar etal., 2002; Chernyshova etal., 2000, 2001).

Thus the aim of the present work is to use the FTIR spectroscopic methods (DRIFT and IRRAS) that can provide information on the presence, interaction, structure and packing of functional groups, and hydrocarbon chains at a surface, and compare the spectroscopic data with the flotation and zeta-potential results and to distinguish the alkyl chain length effect in the coadsorption of long chain amines and alcohols onto silicate surface.

2. EXPERIMENTAL:

2.1. Materials

The pure crystalline quartz and albite mineral samples obtained from Mevior S.A., Greece were used in the present investigations. The chemical analysis showed that quartz was about 99% pure with traces of aluminium (Al_2O_3, 0.1 wt%), calcium (CaO, 0.09 wt%) and iron impurities (Fe_2O_3, 0.046 wt%) and albite more than 98.5% purity with oxides content of 67.9 wt% SiO_2, 19.2 wt% Al_2O_3 and 11.7 wt% Na_2O. The samples were crushed and ground in an agate mortar. The products were wet-sieved to obtain particle size fractions of –150+38 μm and –38 μm. A portion of –38 μm was further ground and micro-sieved in an ultrasonic bath to obtain –5 μm size fraction. The coarser size fraction, –150+38 μm, was employed for Hallimond flotation tests while the fines (–5 μm) were used in zeta-potential and FTIR investigations. The BET specific surface areas for albite coarser and fine fractions were determined to be 0.15 and 2.78 $m^2 g^{-1}$ and the respective specific surface areas for quartz size fractions were found to be 0.09 and 1.30 $m^2 g^{-1}$.

2.2. Reagents

The primary alkyl amines with 99% purity containing C_8, C_{12} and C_{16} chain-lengths were kindly supplied by the Akzo Nobel AB, Sweden. The acetate salts of C_{12} and C_{16} amines were prepared in benzene solvent by mixing equimolar amounts of the respective amine and acetic acid. The acetate salt crystallizes below the freezing temperature and it was purified thrice by recrystallization using fresh benzene each time. The SIGMA spectroscopic grade alcohols of different alkyl chain lengths C_8, C_{10}, C_{12}, C_{14} and C_{16} were purchased from Kebo, Sweden. The pure alcohol solutions were prepared by dissolving the alcohol in ethanol and the resultant aqueous solution of specified concentration contained 5% ethanol. Analar grade NaOH and HCl were used for pH adjustment and deionized water was used in all the experiments.

2.3. Flotation Tests

The single mineral flotation tests were made using Hallimond cell of 100 ml volume. Exactly 1.0 g mineral sample was conditioned first in predetermined concentration of amine solution for 5 min and the suspension was transferred to the flotation cell. The flotation was conducted for 1 min at an air-flow rate of 8 ml min^{-1}. All the tests were performed at a neutral pH region of 6–7.

2.4. Zeta-potential Measurements

Zeta-potentials were determined using a Laser Zee Meter (Pen Kem Inc., model 501) equipped with video system employing a flat rectangular cell. 1.0 g l^{-1} mineral suspension was prepared in 10^{-3} KNO_3 supporting electrolyte solutions, conditioned for 1 hour at room temperature (22°C) in the presence of predetermined concentration of reagents and pH. The pH of the suspension at the time of measurement was reported in the results. After the measurements, the suspension was filtered through millipore filter paper (pore size 0.22 μm) and the solids are air-dried before recording the DRIFT infrared spectrum.

2.5. Diffuse Reflectance FT-IR Measurements

The infrared spectra were registered for all the samples after zeta-potential measurements on the air-dried –5 μm powder. The FTIR spectra were obtained with a Perkin-Elmer 2000 spectrometer with its own diffuse reflectance attachment. Typical spectrum was an average of 200 scans at 4 cm^{-1} resolution with a narrow band liquid nitrogen cooled MCT detector. Since the intensity of the bands with respect to adsorbed layers was low, the samples were not mixed with KBr. The untreated mineral powder was used as reference and the absorbance units were defined by the decimal logarithm of the ratio of initial mineral reflectance to the sample one. The atmospheric water was always subtracted. The area under the alkyl chain bands was measured with the facility available within spectral manipulation.

2.6. Reflectance Absorbance FTIR Measurements

A plate with dimensions of about 20 × 20 mm^2 was cut from a single crystal and the working surface was prepared by polishing successively with the SiC papers down to the 0.25 μm size and washed thoroughly with deionized water. The surface was conditioned with the required reagent solution for about 5 min and the excess solution was removed from the surface with a filter paper. The Infrared Reflection-Absorption Spectra (IRRAS) of the surfactant film at the mineral-air interface were obtained using a Harrick Inc. IRRAS accessory immideately after contact with the solution. All the spectra were collected by coadding 600 scans at 4 cm^{-1} resolution with narrow band liquid nitrogen cooled MCT detector. The angle of incidence of unpolarized radiation was 10°. At this angle practically only the

modes with the Transition Dipole Moment (TDM) parallel to the surface contribute to the IRRAS spectrum and, according to the spectral simulations the absorption bands of adsorbates appear negative (Chernyshova and Rao, 2001a).

2.7. X-ray Photoelectron Spectroscopy (XPS) Measurements

The XPS spectra of quartz powder, albite powder and fractured surfaces, and both the surfaces treated with primary alkyl amines were recorded with AXIS Ultra (Kratos) electron spectrometer under Al monoirradiation and Mg irradiation with sample cooling. The vacuum in the sample analysis chamber during measurements was 10^{-8} Torr. A value of 285.0 eV was adopted as the standard C(1s) binding energy.

3. EXPERIMENTAL RESULTS:

3.1. Hallimond Flotation Studies

The flotation of quartz and albite as a function of C_8, C_{12} and C_{16} amine chlorides at pH 6–7 are shown in Figure 1.

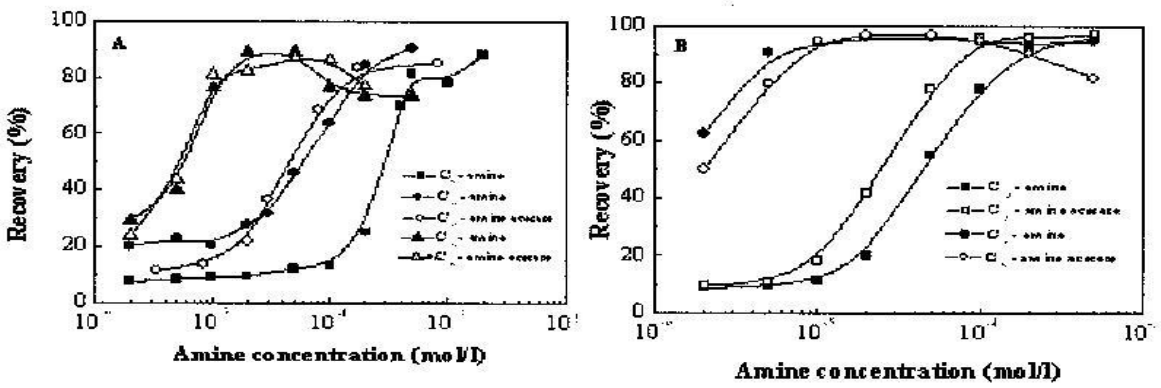

Figure 1. Flotation of quartz (A) and albite (B) with amines as a function of concentration at pH 6–7

The flotation responses with C_{12} and C_{16} amine acetate salts also presented in the same figure. The effect of alkyl chain length on the flotation behaviour of quartz (Figure 1A) observed to be precisely the same as was presented by Fuerstenau *et al.* in 1964. The on-set of hemi-micelle formation for C_8, C_{12} and C_{16} amines corresponds to about 1×10^{-4}, 1×10^{-5} and 2×10^{-6} M respectively illustrating that the critical concentration decreases about one order magnitude with 4 carbons increase in the alkyl chain length. In the case of quartz, the counter ions of amine

appear to have no influence since the flotation response is comparable with amine chloride and acetate solutions. However, the dodecylamine acetate salt gave higher flotation albite recovery than its chloride counter part (Figure 1B), while the other conditions being the same. By outlining the fact that the flotation recovery is not sensitive with surface coverage of collector and one hydrophobic patch on the surface is enough for the particle to adhere air-bubble and float, the effect of acetate ion on amine adsorption cannot be ruled out. Figure 2 shows the effect of alcohol chain length on quartz and albite flotation when it is mixed with C_{12} and C_{16} amine acetate solutions. The results in a mixed composition of a particular C_{12} amine and alcohol concentration as a function of alcohol chain length indicate that the quartz (Figure 2A) flotation reaches maximum at C_{12} alcohol matching to the amine chain length. At alcohol chain length greater than C_{12}, the quartz recovery decreased although insignificantly. The results at the three concentrations of alcohols with varying chain length in the presence of 5×10^{-6} M C_{12} amine demonstrate the same behaviour. The same behaviour of maximum recovery of quartz at the equal chain lengths of amine and alcohol in mixed composition is also observed with C_{16}-amine. However, in this case 80% recovery is almost reached at C_{12} alcohol and attaining to 90% at C_{16}-alcohol. Similar behaviour was observed for albite (Figure 2B). Recognising the fact that the flotation response is not directly related to the degree of collector coverage and thus hydrophobicity, the results signify the alkyl chain length compatibility in mixed surfactant systems on silicate-water interface.The adsorption in a system containing both charged and neutral ions should be greater than one containing only surface active ions, since the neutral molecule heads can actually screen the repulsion between the charged heads of the ions at the interface by co-adsorption between the collector ions. In this aspect, it is worthwhile to remember that the maximum flotation of minerals either with cationic amine or with anionic oleate collector occurs at a pH range where the surfactant exists as ions and neutral molecules Laskowski, 1999; Somasundaran and Ananthapadmanabhan, 1979). This shows the greater surface activity of a neutral molecule in the presence of its ions. Being single surfactant system but existing in neutral and ionic form with the same alkyl chain length, the adsorbed layer could be very packed thereby increasing the surface hydrophobic character and flotation. When the two components differ in chain length, the adsorbed layer expands and the spacing between adjacent molecules is found to increase at the liquid/air interface presumably caused by the thermal motion of the unequal chain lengths in a mixed monolayer (Shah and Shiao, 1975), i.e., formation of gauche defects near the end of chains and longitudinal displacement of the chains. The same phenomena is expected to occur at the solid/liquid interface which explains the observed flotation response of quartz at equal alkyl chain length of amine and alcohol when compared to unequal chain length in mixed composition.

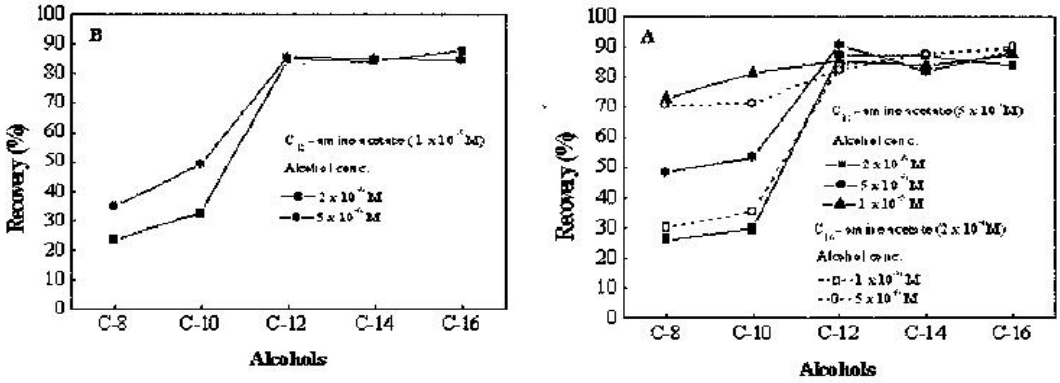

Figure 2. Effect of alkyl chain length in mixed amine/alcohol on quartz (A) and albite (B) flotation at pH 6–7.

3.2. Zeta-potential Studies

In Figure 3, the zeta-potentials of quartz (Figure 3A) and albite (Figure 3B) under identical conditions to that of flotation studies (Figure 1) are presented. For quartz, the hemi-micelle concentration for C_{12} amine is reached at about 4×10^{-4} M and for acetate salt, it corresponds to 7×10^{-4} M. These concentrations are more than one order magnitude higher when compared to flotation recovery curves. Similarly, the critical concentration for C_{16} amine where the zeta-potential raises towards positive is about 2×10^{-5} M in comparison to 1×10^{-6} M where the on-set of flotation is observed.

For C_8 amine, the zeta-potentials are either the same or increased the magnitude of negative charge until 2×10^{-3} M concentration distinguishing that the hemi-micelle concentration is not attained in the concentration range studied. Nevertheless, there is the on-set in flotation with C_8 amine at about 1×10^{-4} M (Figure 1). For albite, the hemi-micelle concentration for C_{12} amine is reached about 1×10^{-4} M and for C_{16} amine is about 8×10^{-6} M. However, a good correlation between the adsorption of amine as evidenced from the area under the alkyl chain bands (3000–2800 cm^{-1}) and zeta-potentials is noticed (Figure 3).

The results show that there is a difference in the critical hemi-micelle concentration (CHC) in the zeta-potential and flotation curves. The difference could be due to the finer and coarser size particles used respectively in these studies. The BET specific surface areas for quartz coarser and fine size fractions were determined to be 0.09 and 1.30 $m^2\ g^{-1}$ and the respective specific surface areas for albite size fractions were found to be 0.15 and 2.78 $m^2\ g^{-1}$.

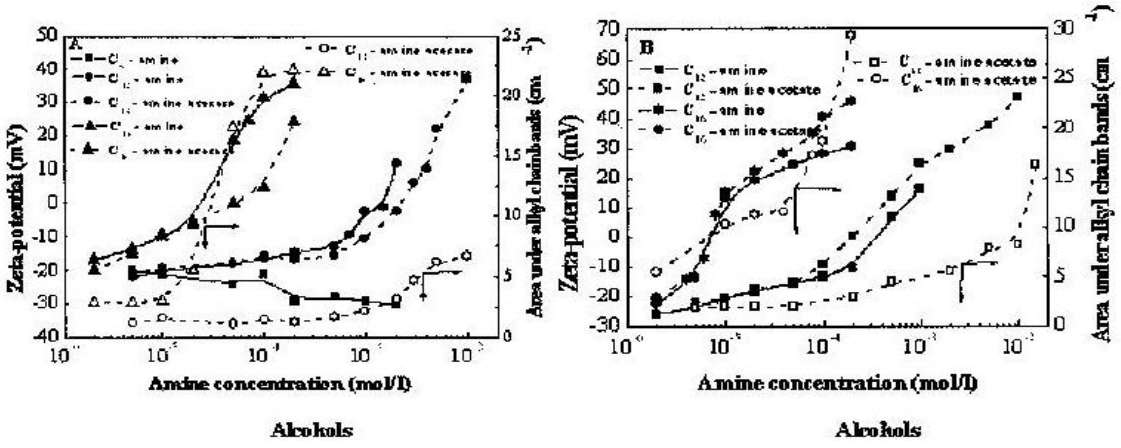

Figure 3. Zeta-potentials of quartz (A) and albite (B) and adsorption of amine as a function of concentration at pH 6–7.

Considering the respective specific surface areas of the two size fractions for quartz and albite, the total surface area involved in either zeta-potential or flotation studies is approximately the same. The good correlation between flotation response, zeta-potential and adsorption density in C_{12} amine/quartz system reported by Fuerstenau [1957], was from the zeta-potentials obtained by streaming potential measurements using coarser particles.

In the case of quartz, the onset amine concentration (CHC) of the steep increase in the zeta-potential curves with amines and their salts is varied with the acetate salt occurring at a slightly higher concentration. The co-adsorption of acetate ion would suppress the adsorption of amine so that the CHC for the ammonium acetate salt attains at a higher bulk amine concentration. The infrared studies presented later showed that acetate ions are adsorbed on quartz surface. The adsorption of acetate ions on a silicate surface through hydrogen and chemical bonding was reported (Kubicki etal., 1999).

The zeta-potentials of quartz and microcline in mixed amine–alcohol solution at two total concentrations composing 1:1 concentration ratio is depicted in Figure 4. The results as a function of increasing alcohol chain length but at a constant chain length of amine reveal that the quartz (Figure 4A) and microcline (Figure 4B) possess lesser negative potential in a system when the alkyl chain lengths of amine and alcohol are the same. The concentrations used in these studies are well below the critical hemi-micelle concentration as elucidated from Figure 2 and this is because of low solubility of alcohols and thus the difficulty to prepare higher concentration solutions.

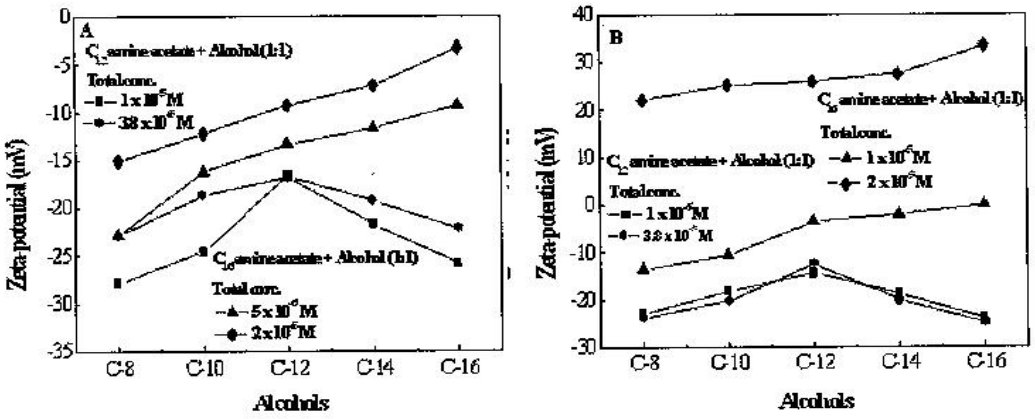

Figure 4. Effect of alkyl chain length in mixed amine–alcohol on (A) quartz and (B) microcline zeta-potential at pH 6–7.

Nonetheless, the lesser negative potential at equal chain lengths indicate more adsorption of amine in comparision to other alkyl chain length manifesting closer packing of molecules at equal chain lengths. Although, measurements have not made with alcohols greater than C_{16} chain lengths in the presence of C_{16} amine due to to negligible solubility, a decrease in zeta-potential is expected beyond C_{16} alcohol chain length.

3.3 Infrared Diffuse Reflectance Spectral Studies

The reference DRIFT spectra of dodecyl amine, its acetate salt, and dodecyl alcohol are shown in Figure 5. The bands characteristic of alkyl chains, $\nu_{as}(CH_3)$, $\nu_{as}(CH_2)$, and $\nu_s(CH_2)$ groups, for dodecyl amine are identified at 2956, 2920 and 2852.5 cm^{-1} respectively (Bellamy, 1975). The corresponding bands for its acetate salt are observed at 2950, 2921.6 and 2851.6 cm^{-1}. However, the spectrum of acetate salt is composed of several other bands (i.e., 2963, 2933, 2900, 2890 and 2870.7 cm^{-1}) in the alkyl chain region owing to the acetate ion and probably to another packing of C-H chains in the amine acetate crystallites. A sharp intensity band at 3333 cm^{-1} in the amine spectrum is due to $\nu_{as}(NH_2)$ and $\nu_s(NH_2)$, while in the case of acetate salt two broad bands at 3000 and 2600 cm^{-1} are observed, which are assigned to $\nu_{as}(NH_3^+)$ and $\nu_s(NH_3^+)$ respectively (Bellamy, 1975; Koretsky etal., 1997; Przeslawska etal., 1999). The reference spectra show that the amine molecule in the bulk phase in neutral and protonated forms can be identified with the appearance and disappearance of the band at 3333 cm^{-1}. The dodecyl alcohol spectra show a broad band centering around 3318 cm^{-1} characteristic of the H-bonded OH...O of ν(OH) group (Bellamy, 1975), in addition to the bands characterizing alkyl chains. The spectra also display several bands in the region 1750-1000 cm^{-1} but in the same region quartz exhibits strong absorption bands and thus difficult to identify any bands under mono- or submono-layer adsorption. Thus

this region is not comprehensible in the present investigations because of the low surfactant concentrations employed.

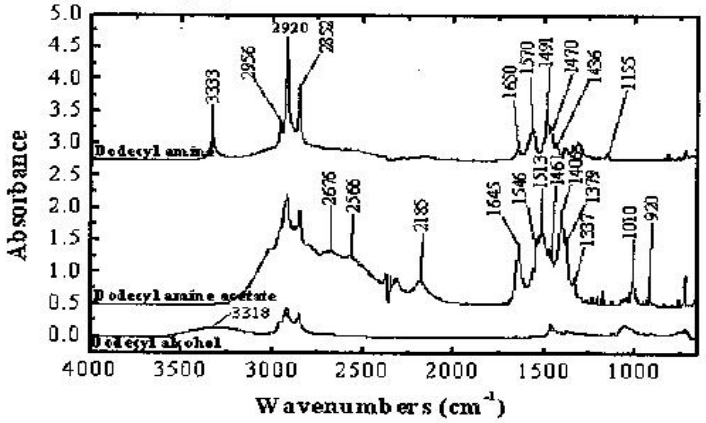

Figure 5. DRIFT spectra of dodecyl alcohol, dodecyl amine acetate and dodecyl amine.

The DRIFT spectra of quartz and albite powder conditioned in 1:1 mixed solutions of alkyl ammonium acetate and alkyl alcohol of different chain lengths at a total concentration of 1×10^{-5} M are shown in Figs. 6 and 7 respectively. The reference quartz spectrum (Figure 6a, curve 0) show a narrow band at 3745 cm^{-1} due to OH stretching vibrations of surface isolated silanol groups and the complex absorption band in the region 3000-3700 cm^{-1} is due to adsorbed H-bonded hydroxyls and water (Koretsky etal., 1997). The reference albite spectrum shown in (Figure 7a, curve 3) was used as adsorbent. The H-bonded hydroxyls, which are predominantly attached to Si rather than Al surface atoms on the albite surface, and physically adsorbed water are responsible for the broad band centered at 3300 cm^{-1} (Koretsky etal., 1997; Kubicki etal., 1999).

The spectra of quartz conditioned with mixed solutions of C_{16} amine acetate–C_{12} alcohol and with reverse chain lengths (Figure 6a, curves 1 and 2), and binary solutions of C_{16} amine acetate–C_8 alcohol and reverse chain lengths (Figure 6b, curves 1 and 2) and similarly for albite i.e, Figure 7a, curves 1 and 2 and Figure 7b, curves 1 and 2, display characteristic alkyl chain length bands due to adsorbed surfactants. The intensities of the CH stretching bands are nearly the same within the experimental error for the reverse chain lengths illustrating that the quantity of adsorbed surfactants is the same. However, the adsorbed amount increased for the amine–alcohol pair when the sum chain length is more which is in agreement with the general tendency of increasing adsorption with increasing alkyl chain length.

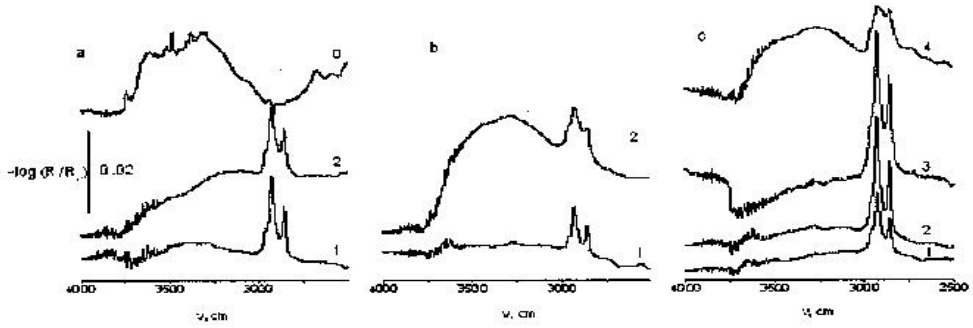

Figure 6. DRIFT spectra of (a, curve 0) initial quartz and the quartz conditioned in the 1:1 binary solutions (pH 6–7) of alkyl ammonium acetate and alkyl alcohol of different chain lengths at total concentration of 1×10^{-3} M. The component chain lengths are as follows. (a) 1, C_{16} amine–C_{12} alcohol; 2, C_{12} amine–C_{16} alcohol. (b) 1, C_{16} amine–C_8 alcohol; 2, C_8 amine–C_{16} alcohol. (c) 1, C_{16} amine–C_{16} alcohol; 2, C_{12} amine–C_{12} alcohol. For comparison, the quartz conditioned in the solutions of the pure (3) HAAc and (4) C_{16} alcohol. The absorbance scale is the same for all the graphs.

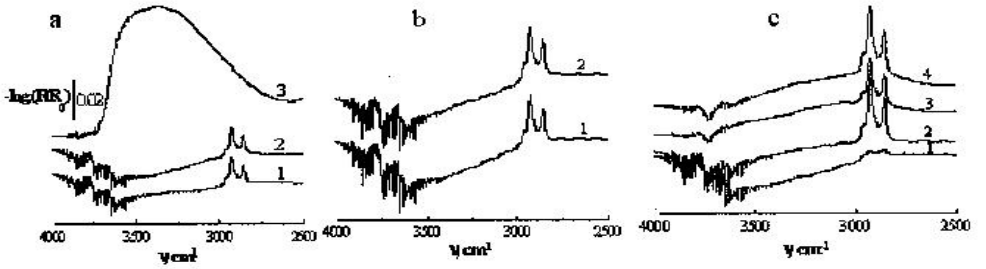

Figure 7. DRIFT spectra of (a, curve 3) initial albite measured against KBr and the albite conditioned 10 min in the 1:1 binary solutions (pH 6–7) of alkyl ammonium acetate and alkyl alcohol of different chain lengths at a total concentration of 1×10^{-3} M. The component chain lengths are as follows. (a) 1, C_{16} amine–C_{12} alcohol; 2, C_{12} amine–C_{16} alcohol. (b) 1, C_{16} amine–C_8 alcohol; 2, C_8 amine–C_{16} alcohol. (c) 1, C_{12} amine–C_{12} alcohol; 2, C_{16} amine–C_{16} alcohol. For comparision, the albite conditioned in the solutions of the pure (3) C_{16} amine acetate and (4) C_{16} alcohol. The absorbance scale is the same for all the graphs.

When the CH stretching band intensities of the adsorbed pure amine and alcohol (Figure 6c, curves 3 and 4) are compared, the adsorbed amine is approximately three times larger than that of alcohol at the same alkyl chain length. In the case of competitive adsorption of monomers from the binary solutions of amine and alcohols with the reverse chain lengths, the surface coverage is expected to be larger for a mixture with longer amine homologues. However, if the adsorbed species are the 1:1 solvated associates, the surface coverage should be similar, which is observed. It could be that these solvated associates are the ion-molecule pairs where the alcohol hydroxyls act as base while the ammonium head group

behaves as acid. Such dimers have been suggested to be formed between the protonated amine and alcohol (Somasundaran and Ananthapadmanabhan, 1979).

The intense negative band at 3745 cm^{-1} due to free silanols in the spectrum of the quartz conditioned with the solution of the pure amine (Figure 6c, curve 3) and similarly for albite (Figure 7c, curve 3) diminishes in the case of co-adsorption and totally disappears for pairs C_{12} amine–C_{16} alcohol and C_8 amine–C_{16} alcohol. Since the negative intensity of the silanol band arises from the interaction of silanols with the adsorbate as explained earlier (Vidyadhar etal., 2002), the free silanols are less involved in the co-adsorption and as well in the adsorption of the alcohol, when compared to the adsorption of pure amines. The interaction mechanism of mixed alkyl amine and alcohol on silicate surface with structural disposition has been reported by Chernyshova and Hanumantha Rao [2001b].

The DRIFT spectra adsorption results of quartz and albite with C_{16} amines are presented in Figure 8. Although the CH_2 peak area curves characterizing the adsorbed amine appear to be the same with increasing concentration until the break corresponding to the onset of CHC, the negative silanol groups area increases. This increase in negative area reached maximum at a certain bulk amine concentration. It signifies that the surface silanol groups are diminished because of the interaction with silanol groups. The bulk amine concentration until which the silanol groups are affected and the break in the adsorption curve, i.e., CHC, are found to be different in the case of amine and amine acetate. It suggests the influence of acetate counter ion on amine adsorption.

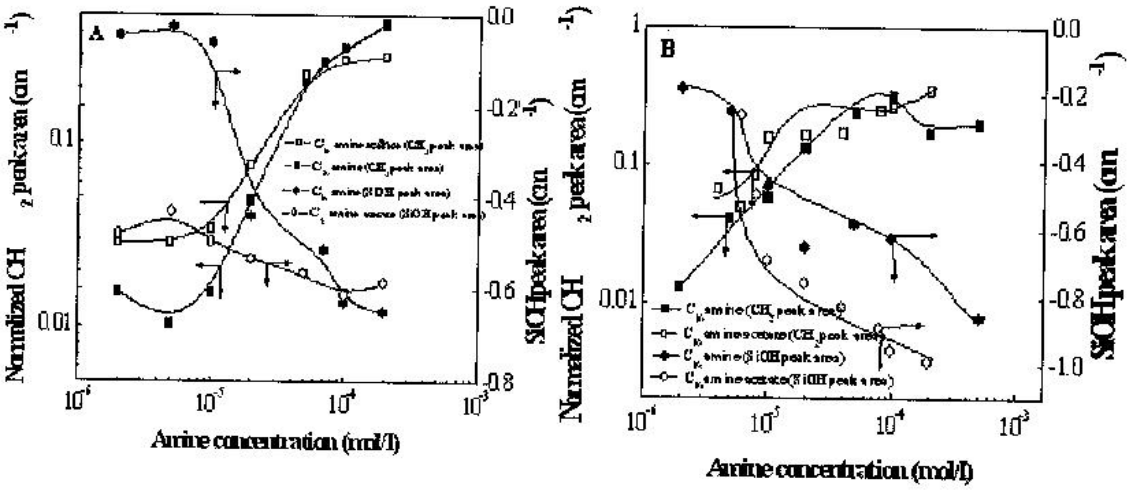

Figure 8. Influence of C_{16} amine adsorption on quartz (A) and albite (B) silanol groups

3.4 Infrared Reflection Absorption Spectral studies

It is well established in numerous studies [(Horn, 1998; Mendelsohn and Brauner, 1995) that the frequencies of the CH_2 and CH_3 stretching bands of hydrocarbon chains are extremely sensitive to the conformational ordering of the chains in a layer. When the chains are highly ordered (all-*trans* Zigzag conformation), the narrow absorption bands appear at 2918 (CH_2^{asym}) and 2848 cm^{-1} (CH_2^{sym}) in the infrared spectrum of the layer. On the other hand, if conformational disorder is included in the chains, they shift upward to 2926 and 2856 cm^{-1}, depending upon the gauche conformers in the average orientation. Although these frequency shifts are small, modern FTIR spectrometers permit their routine determination with a precision of better than ± 0.1 cm^{-1}. It was found that generally the hydrocarbon order decreases with decreasing chain length (Park and Franses, 1995). Another important characteristic of the molecule organisation in a layer is the absorption bandwidth, which is proportional to the degree of the molecule mobility within the layer. It was found that the bandwidth increases with temperature when the chain packing disorder increases (Katayama etal., 1993).

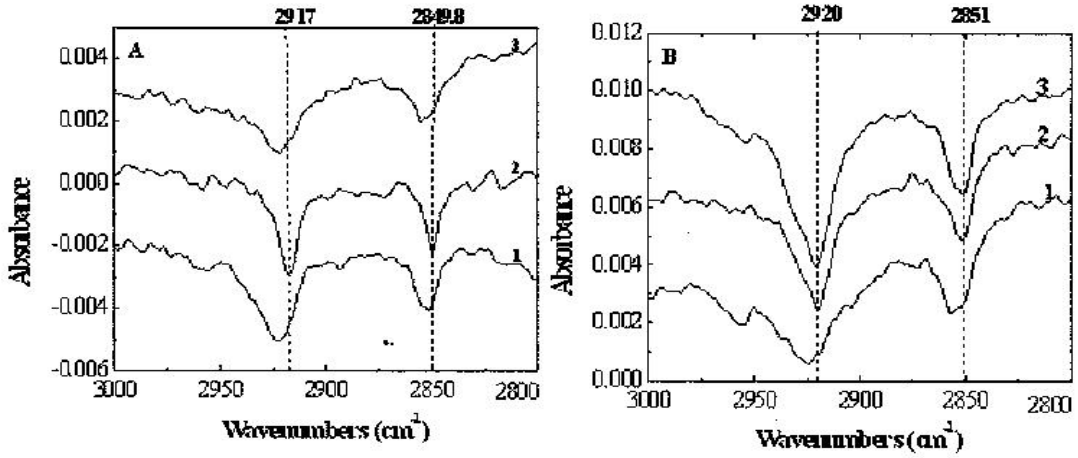

Figure 9. IRRAS spectra of (A) quartz and (B) albite surface after 5-min conditioning in a 1:1 solution of dodecyl amine and (1) octyl alcohol, (2) dodecyl alcohol, and (3) hexadecyl alcohol with the total concentration 2×10^{-5} M at natural pH.

Figure 9 shows the IRRAS spectra in the stretching C-H mode region of dodecyl amine coadsorbed with long-chain alcohols of 8, 12, and 16 carbons on quartz (Figure 9A) and albite (Figure 9B) from the 1:1 aqueous (natural pH) solutions of the total concentration 2×10^{-5} M. All the spectra display the distinct CH_2^{asym} and CH_2^{sym} bands. Importantly that the lowest frequencies and the

narrowest widths of these bands are exhibited by the spectrum of dodecyl amine coadsorbed with dodecyl alcohol. This observation testifies to the highest order and packing of the adsorbed species, when the chain lengths of the coadsorbents are equal and can be regarded as a spectroscopic confirmation of the results of the surface force measurements by Yoon and Ravishankar (1994, 1996). They found that the coadsorption of dodecyl amine with dodecyl alcohol on mica yields the most hydrophobic effect (the strongest hydrophobic force) as compared to the other cases studied. Using the molar absorptivity of the hydrocarbon chains, the coverage by the adsorbed molecules was roughly estimated to be equal to about 0.5 monolayer in all the cases considered (Vidyadhar and Rao, 2007; Vidyadhar etal., 2002; Chernyshova etal., 2000, 2001).

3.5. XPS Studies

Figure 10 shows the N(1s) spectra of the quartz powder treated with 4×10^{-5} and 2×10^{-4} M C_{12} amine acetate, and 2×10^{-4} M C_{12} amine. At amine concentration below CHC (curve 3), the spectrum is composed of one component at 400.1 eV. The spectra exhibit two components of N(1s) peak at CHC with binding energies of 399.5 eV and 401.5 eV. Similarly, the N(1s) spectrum of the albite conditioned in the 4×10^{-5} M solutions of C_{12} amine consists of a single peak at 401.4 eV and in the case of C_{12} amine acetate, a peak at 400.9 eV with a small satellite at 398.8 eV (Figure 11). While at a higher concentration (2×10^{-4} M) two N (1s) peaks 399.8 ± 0.1 and 401.2 ± 0.1 eV are present. These values, respectively, correspond to the binding energies of amino and ammonium groups when compared to the spectra of crystalline C_{12} amine and C_{12} amine acetate (Vidyadhar etal., 2002). Thus, the adsorbed layer is composed of molecular alkyl amine and alkyl ammonium ions. The adsorption of amine on silanol groups can be realized with the amino group H-bonded to surface silanol attributed to the first component while the second component is attributed to the ammonium group formed owing to a charge transfer in strong H-bond between nitrogen of the amino and silanol groups (Vidyadhar and Rao, 2007; Vidyadhar etal., 2002; Chernyshova etal., 2000, 2001):

$$\equiv SiOH\ldots H_2N\text{-}R \Leftrightarrow \equiv SiO^{-}\ldots H_3^{+}N\text{-}R \qquad (1)$$

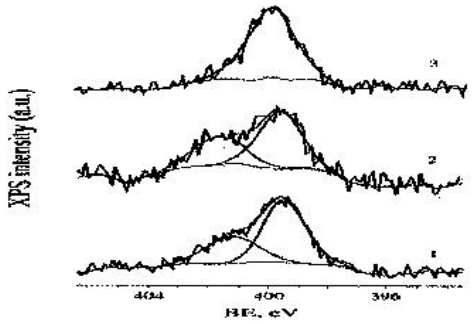

Figure 10. XPS N(1s) spectra of quartz powder conditioned with (1) 2×10^{-4} M C_{12} amine; (2) 2×10^{-4} M C_{12} amine acetate; and (3) 4×10^{-5} M C_{12} amine acetate.

The above equilibrium exists at the interface once the molecular amine appears at the surface corresponding to CHC. The single peak for quartz and albite at concentrations less than CHC at 400.1 and 401.1 ± 0.3 eV respectively (Figs. 10 and 11) can thus be characterised by the ammonium group H-bonded to the silanols as:

$$\equiv Si - O \ldots H - {}^{+}NH_2 - R \qquad (2)$$

The NH...O bonds are weaker than the N...HO bonds and proton donating property of surface silanol groups is higher than its proton-accepting property in the H-bonding with a water molecule and acetic acid/acetate ion pair (Pimentel and Mc Clellan, 1960). The transition from Eq (2) to Eq (1) is observed from infrared spectra where the broad band is centred at 3250 cm^{-1} at < CHC and shifting to 3000 cm^{-1} at > CHC. It is well known that a red shift of any H-bonded stretching mode points to the H-bond strengthening. Thus, the transition from Eq (2) to Eq (1) while strengthening H-bond occurring at CHC supports the above assignment of the N(1s) spectra.

Thus, the extensively cited three regions of adsorption (Somasundaran and Fuerstenau, 1966) can further be exemplified that i) An amine cation is H-bonded to surface silanol groups and this bond becomes stronger after the break in the adsorption characteristics (isotherm, zeta-potential, flotation); ii) at the break the origin of the adsorbed amine species changes qualitatively, and the molecular amine species appear together with an alkyl ammonium ion attached to deprotonated silanol group and thereby forming monolayer- thick patches of well-oriented and densely packed adsorbed amine species, rendering the surface highly hydrophobic; and iii) at higher amine concentration, bulk precipitation of amine takes place.

4. ADSORPTION MECHANISM:

The hemi-micelle model cannot explain the presence of neutral amine molecules in the adsorbed film below monolayer coverage and a strong H-bonding between amino head groups and the surface silanols. The present results can be interpreted within the framework of a two-dimensional condensation model if one substitutes the precipitation phenomena in place of condensation phenomena. However, before the transition to increased adsorption, the ammonium groups are hydrogen bonded to the negatively charged silanols (Eq (2)), and when the local concentration at the interface approaches a critical value, the adsorbed layer transforms into crystalline state owing to precipitation of neutral amine. At the first step, the process is two-dimensional and the adsorbed neutral amine establishes the equilibrium shown in Eq (1). Screening the electrostatic repulsion between head groups, the neutral molecules change the structure of the adsorbed layer substantially, increasing the density of the monolayer. The second phase transition of three-dimensional precipitation occurs when the bulk solubility limit is reached at the surface. This adsorption model is illustrated in Figure 12 (Chernyshova et al., 2000, 2001).

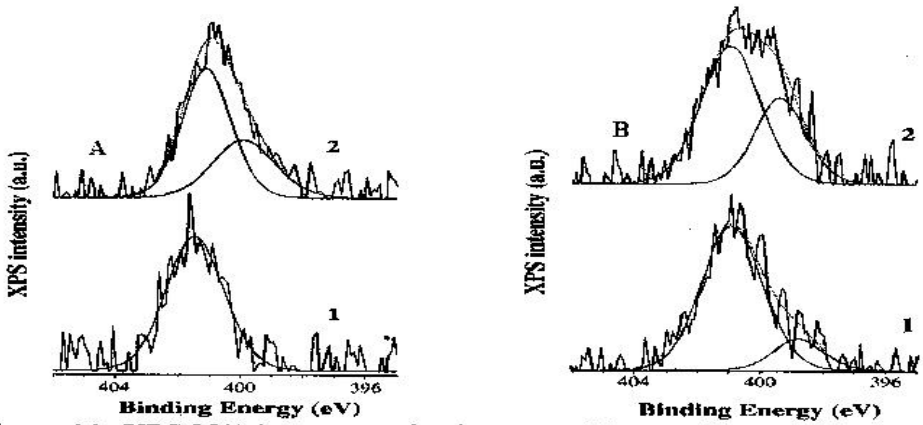

Figure 11. XPS N(1s) spectra of a fracture albite surface conditioned in a solution (pH 6.5) of C_{12} amine acetate (A) and C_{12} amine (B). The amine concentrations are (1) 4×10^{-5} M; and (2) 2×10^{-4} M.

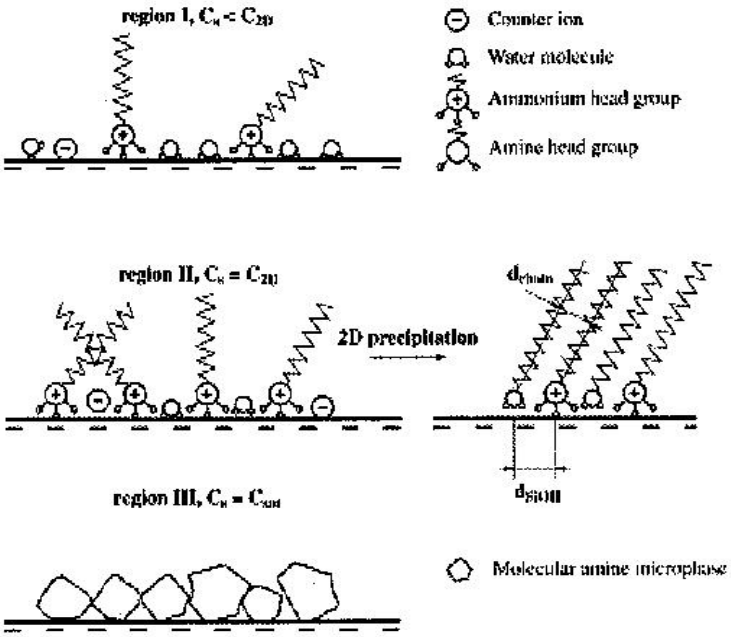

Figure 12. Adsorption according to the 2D-3D precipitation mechanism

5.CONCLUSIONS :

The infrared spectra showed that at low bulk amine concentrations, the surface silanol groups interact with ammonium groups through hydrogen bonds.

After hemimicelle concentration, the XPS spectra showed neutral amine molecules along with the protonated ammonium ions coordinated to deprotonated silanol oxygen anions on the surface. Because of this adsorption steeply increases. At higher concentrations, the molecular amine precipitates on the surface. The later two regions of adsorption, where formation of neutral amines takes place, is affected by the acetate counterions.

When the alkyl chain lengths of mixed amine and alcohol are the same, the adsorbed layer on silicate surface is closely packed leading to enhanced hydrophobicity and thus maximum flotability.

The total concentration in mixed composition is reduced to one order magnitude when compared to the amine concentration alone for achieving the same flotation response. The neutral molecule coadsorption in between charged amine heads shielded its repulsion and thereby the adsorption is increased owing to lateral tail-tail hydrophobic bonds.

At equal alkyl chain lengths of amine and alcohol, the zeta-potentials are less negative manifesting more adsorption of amine owing to closer packed layer.

The CH_2^{asym} and CH_2^{sym} bands in reflection-absorption spectroscopy spectra occurred at the lowest frequencies with the narrowest widths when the coadsorbents were dodecyl amine and dodecyl alcohol, validating the highest order and packing of the adsorbed species at equal alkyl chain lengths.

The results are interpreted in terms of successive two-dimensional and three-dimensional precipitation of amine on silicate surface.

REFERENCES:

Bellamy L.J., 1975, *The Infrared Spectra of Complex Molecules*. Wiley, New York.

Chernyshova I. V.; Hanumantha Rao K.; Vidyadhar A.; Shchukarev A.V., 2000, *Mechanism of Adsorption of Long-Chain Alkylamines on Silicates. A Spectroscopy Study. 1. Quartz*, Langmuir 16, 8071-8084.

Chernyshova I.V.; Hanumantha Rao K.; Vidyadhar A.; Shchukarev A.V., 2001, *Mechanism of Adsorption of Long-Chain Alkylamines on Silicates. A Spectroscopy Study. 2. Albite*, Langmuir 17, 775-785.

Chernyshova I.V.; Hanumantha Rao K., 2001a, *A New Approach to the IR Spectroscopic Study of Molecular Orientation and Packing in Adsorrbed Monolayers. Orientation and Packing of Long-Chain Primary Amines and Alcohols on Quartz*, J. Phys. Chem. *B*. 105, 810-820.

Chernyshova I.V.; Hanumantha Rao K., 2001b, *Mechanism of Coadsorption Long-Chain Alkylamines and Alcohols on Silicates. Fourier Transform Spectroscopy and X-ray Photoelectron Spectroscopy Studies*, Langmuir 17, 2771-2719.

Fuerstenau D.W., 1957, Correlation of Contact Angles, *Adsorption Density, Zeta Potentials, and Flotation Rate*, Min. Eng. 208, 1365-1367.

Fuerstenau D.W.; Healy T.W.; Somasundaran P., 1964, *The Role of Hydrocarbon Chain of Alkyl Collectors in Flotation*, Trans. SME/AIME, vol.229, 321-325.

Fuerstenau D.W.; Jang H.M.," 1991, Langmuir, vol.7, 3138.

Fuerstenau D.W.; Raghavan S., 1980, *The Crystal Chemistry, Surface Properties and Flotation Behaviour of Silicate Minerals*, Proc." Int. Miner. Process. Congr"., Vol. II, D.N.P.M., Sao Paulo, 368-415.

Gaudin A.M.; Fuerstenau D.W., 1955, *Quartz Flotation with Cationic Collectors*, Trans. Soc. Min. Eng. AIME. vol.202, 958-962.

Horn A., 1998, *Infrared Spectroscopic Techniques for the Study of Thin interfacial Films Clark R.J.H.; Hester R.E. (Eds.)*, A Spectroscopy for Surface Science. Vol. 26, John Wiley and Sons, New York, 273-339.

Katayama N.; Enomoto S.; Satao T.; Ozaki Y.; Kuramoto N., 1993, *J. Chem. Phys.* 97, 6880-6884.

Koretsky C.M.; Sverjensky D.A.; Alisbury J.W.; D'Aria D.M., 1997, *Detection of Surface Hydroxyl Species on Quartz, γ-Alumina, and Feldspars using Diffuse Reflectance Infrared Spectroscopy*, Geochim. Cosmochim. Acta. 61, 2193-2210.

Kubicki J.D.; Schroeter L.M.; Itih M.J.; Nguyen B.N.; Aptiz S.E., 1999, *Attenuated Total Reflectance Fourier-Transform Infrared Spectroscopy of Carboxylic Acids onto Mineral Surfaces,* Geochim. Cosmochim. Acta. 63, 2709-2725.

Laskowski J. S., 1999, *Weak Electrolyte Collectros*, Advances in Flotation Technology, B.K. Parekh and J.D. Miller (Eds.), SME/AIME, Denver, Colorado, 59-82.

Leja J., 1982, *Surface Chemistry of Froth Flotation*, Plenum Press, New York. Mendelsohn, R., Brauner, J.W. and Gericke, A., 1995, *Ann. Rev. Phys. Chem.* 46, 305-334.

Park S.Y.; Franses E., 1995, *Langmuir* 11, 2187-2194.

Pimentel, G.C and A.L. Mc Clellan, A.L., 1960, *The Hydrogen Bond*, Freeman, SanFrancisco.

Przeslawska M.; Melikowa S.M.; Lipkowski P.; Koll A., 1999, *Gas Phase FT-IR Spectra and Structure of Aminoalcohols with Intramolecular Hydrogen Bonds. I. The Shape of the ν(OH) Vibrational Bands in $R_2NC_3H_6OH$ (R=H, CH_3)*, Vibrational Spectroscopy. 20, 69-83.

Shah D.O.; Shiao S.Y., 1975, *Monolayers, Advances in Chemistry Series 144*, E.D. Goddard (Ed.), American Chemical Society, Washington D.C, , 153 164.

Smith R.W.; Scott J.L., 1990, *Mechanisms of Dodecylamine Flotaion of Quartz*, Miner. Process. Ext. Metall. Rev. vol.7, 81-94.

Somasundaran P.; Ananthapadmanabhan K.P., 1979, *Solution Chemistry of Surfactants and the Role of it in Adsorption and Froth Flotation in Mineral Water Systems*, Solution Chemistry of Surfactants, K.L. Mittal (Ed.), Vol. 2, 777-800, Plenum Press, New York.

Somasundaran P.; Fuerstenau D.W., 1996, *Mechanisms of Alkylsulfonate Adsorption at the Alumină-Water Interface*, J. Phys. Chem., vol.79, 90-97.

Vidyadhar A.; Hanumantha Rao K.; Chernyshova I.V.; Pradip and Forssberg, K.S.E., 2002, J. Colloid Interface Sci., vol.256, 59-72.

Vidyadhar A.; Hanumantha Rao K., 2007, *Adsorption Mechanism of Mixed Cationic/Anionic Collectors in Feldspar-Quartz Flotation System*, J. Colloid Interface Sci., vol.306, 195-204.

Yoon R.H.; Ravishankar S.A., 1994, *J. Colloid Interface Sci.* 166, 215-224.

Yoon R.H.; Ravishankar S.A., 1996, *J. Colloid Interface Sci.* 179, 319-402.